ELASTIC STRESS FIELDS IN THE VICINITY OF A NARROW NOTCH WITH CIRCULAR ROOT

G. Kullmer*

Using an Airy's stress function, stress field equations for general plane loading, valid for a slit ending in a drilled hole, are derived. The appropriate solution for antiplane–loading is found by using the hydrodynamic analogy to torsion and considering the flow past a circular cylinder. The stress distribution is described with the stress intensity factors K_I, K_{II}, and K_{III} in a form similar to the well–known Creager–equations, which are valid for parabolic notches. Neglecting all terms depending on notch root radius, the solution of the sharp crack equivalent is obtained.

INTRODUCTION

Very often the stress distribution in the vicinity of cracklike narrow notches with notch root radius ρ and notch depth a ($\rho << a$) is estimated with the Creager–equations (1), which read in cylindrical coordinates –position of the origin of the coordinate system see Fig. 1– for general plane loading

$$\sigma_r = \frac{K_I}{4\sqrt{2\pi r}}\left[(5-\frac{2\rho}{r})\cos\frac{\varphi}{2}-\cos\frac{3\varphi}{2}\right]-\frac{K_{II}}{4\sqrt{2\pi r}}\left[(5+\frac{2\rho}{r})\sin\frac{\varphi}{2}-3\sin\frac{3\varphi}{2}\right],$$

$$\sigma_\varphi = \frac{K_I}{4\sqrt{2\pi r}}\left[(3+\frac{2\rho}{r})\cos\frac{\varphi}{2}+\cos\frac{3\varphi}{2}\right]-\frac{K_{II}}{4\sqrt{2\pi r}}\left[(3-\frac{2\rho}{r})\sin\frac{\varphi}{2}+3\sin\frac{3\varphi}{2}\right], \quad (1a)$$

$$\tau_{r\varphi} = \frac{K_I}{4\sqrt{2\pi r}}\left[(1+\frac{2\rho}{r})\sin\frac{\varphi}{2}+\sin\frac{3\varphi}{2}\right]+\frac{K_{II}}{4\sqrt{2\pi r}}\left[(1-\frac{2\rho}{r})\cos\frac{\varphi}{2}+3\cos\frac{3\varphi}{2}\right],$$

and for antiplane–loading

$$\tau_{rz} = \frac{K_{III}}{\sqrt{2\pi r}}\sin\frac{\varphi}{2}, \quad \tau_{\varphi z} = \frac{K_{III}}{\sqrt{2\pi r}}\cos\frac{\varphi}{2}. \quad (1b)$$

Since for $\rho << a$ K_I, K_{II}, and K_{III} are the stress intensity factors of the sharp crack equivalent (i.e. crack of the same orientation and length as the notch in question), for $\rho/r \rightarrow 0$ the stress field equations for the crack are obtained.

* Institute of Applied Mechanics, University of Paderborn, FRG

The Creager–equations are the theoretical background of many experimental and numerical investigations concerning blunt cracks. Although it can easily be shown, that they are only valid for parabolic notches (Fig. 1) the model notches applied in such studies are in most cases U–shaped notches or slits ending in a drilled hole (Fig. 2). Therefore, it is the aim of this work to derive new stress field equations, valid for narrow notches with circular root, in a form similar to the Creager–equations.

METHOD OF SOLUTION

The Plane Problem

For a disk with a straight slit ending in a circular hole (Fig. 2) under general plane loading the following Airy's stress function is proposed:

$$A = (C_1 r^{\frac{3}{2}} + C_2 r^{\frac{1}{2}} + C_3 r^{-\frac{1}{2}}) \cos\frac{\varphi}{2} + (C_4 r^{\frac{3}{2}} + C_5 r^{\frac{1}{2}} + C_6 r^{-\frac{3}{2}}) \cos\frac{3\varphi}{2}$$
$$+ (D_1 r^{\frac{3}{2}} + D_2 r^{\frac{1}{2}} + D_3 r^{-\frac{1}{2}}) \sin\frac{\varphi}{2} + (D_4 r^{\frac{3}{2}} + D_5 r^{\frac{1}{2}} + D_6 r^{-\frac{3}{2}}) \sin\frac{3\varphi}{2} . \quad (2)$$

The stress components may be calculated with the following definitions:

$$\sigma_r = \frac{1}{r^2}\frac{\partial^2 A}{\partial \varphi^2} + \frac{1}{r}\frac{\partial A}{\partial r} , \quad \sigma_\varphi = \frac{\partial^2 A}{\partial r^2} , \quad \tau_{r\varphi} = -\frac{1}{r}\frac{\partial^2 A}{\partial r \partial \varphi} + \frac{1}{r^2}\frac{\partial A}{\partial \varphi} . \quad (3)$$

For mode I–loading only the symmetrical terms of equation (2)

$$A_I = (C_1 r^{\frac{3}{2}} + C_2 r^{\frac{1}{2}} + C_3 r^{-\frac{1}{2}}) \cos\frac{\varphi}{2} + (C_4 r^{\frac{3}{2}} + C_5 r^{\frac{1}{2}} + C_6 r^{-\frac{3}{2}}) \cos\frac{3\varphi}{2} , \quad (4)$$

stated by Neuber (2) for tensile loading, need to be considered. To satisfy the boundary conditions for a stress–free circular notch surface

$$\sigma_r(r = \rho) = 0 , \quad \tau_{r\varphi}(r = \rho) = 0 , \quad (5)$$

the constants are chosen

$$C_2 = -2\, C_1 \rho , \quad C_3 = C_1 \rho^2 , \quad C_5 = -\frac{3}{2} C_4 \rho , \quad C_6 = \frac{1}{2} C_4 \rho^3 . \quad (6)$$

The boundary conditions along the slit require, that σ_φ and $\tau_{r\varphi}$ vanish for $\varphi = \pm \pi$. This is satisfied for σ_φ, but for $\tau_{r\varphi}$ this is only approximately possible. To assure, that the main portion of shear stresses vanishes along the slit, for the limiting case $\rho/r \longrightarrow 0$ the solution of the sharp crack equivalent is demanded. Thus, the comparison with equations (1) yields

$$C_1 = 3\, C_4 = \frac{K_I}{\sqrt{2\pi}} , \quad (7)$$

and for mode I–loading the following stress field equations are obtained:

$$\sigma_r = \frac{K_I}{4\sqrt{2\pi r}}\left\{\left[5-2\frac{\rho}{r}-3\left[\frac{\rho}{r}\right]^2\right]\cos\frac{\varphi}{2}-\left[1-\frac{7}{2}\frac{\rho}{r}+\frac{5}{2}\left[\frac{\rho}{r}\right]^3\right]\cos\frac{3\varphi}{2}\right\},$$

$$\sigma_\varphi = \frac{K_I}{4\sqrt{2\pi r}}\left\{\left[3+2\frac{\rho}{r}+3\left[\frac{\rho}{r}\right]^2\right]\cos\frac{\varphi}{2}+\left[1+\frac{1}{2}\frac{\rho}{r}+\frac{5}{2}\left[\frac{\rho}{r}\right]^3\right]\cos\frac{3\varphi}{2}\right\}, \quad (8)$$

$$\tau_{r\varphi} = \frac{K_I}{4\sqrt{2\pi r}}\left\{\left[1+2\frac{\rho}{r}-3\left[\frac{\rho}{r}\right]^2\right]\sin\frac{\varphi}{2}+\left[1+\frac{3}{2}\frac{\rho}{r}-\frac{5}{2}\left[\frac{\rho}{r}\right]^3\right]\sin\frac{3\varphi}{2}\right\}.$$

In order to solve the mode II–problem the antisymmetrical terms

$$A_{II} = (D_1 r^{\frac{3}{2}} + D_2 r^{\frac{1}{2}} + D_3 r^{-\frac{1}{2}})\sin\frac{\varphi}{2} + (D_4 r^{\frac{3}{2}} + D_5 r^{\frac{1}{2}} + D_6 r^{-\frac{3}{2}})\sin\frac{3\varphi}{2} \quad (9)$$

of equation (2) are convenient. The boundary conditions (eqs (5)) yield

$$D_2 = -2D_1\rho, \quad D_3 = D_1\rho^2, \quad D_5 = -\frac{3}{2}D_4\rho, \quad D_6 = \frac{1}{2}D_4\rho^3. \quad (10)$$

Along the slit $\tau_{r\varphi}$ is zero, whereas, the boundary condition $\sigma_\varphi(\varphi = \pm\pi) = 0$ can only approximately be satisfied. The main portion of σ_φ vanishes, if for the limiting case $\rho/r \longrightarrow 0$ the solution of the sharp crack equivalent is required. Thus, the comparison with equations (1) results in

$$D_1 = D_4 = \frac{-K_{II}}{\sqrt{2\pi}}, \quad (11)$$

and the stress field equations for mode II–loading read:

$$\sigma_r = \frac{-K_{II}}{4\sqrt{2\pi r}}\left\{\left[5-2\frac{\rho}{r}-3\left[\frac{\rho}{r}\right]^2\right]\sin\frac{\varphi}{2}-\left[3-\frac{21}{2}\frac{\rho}{r}+\frac{15}{2}\left[\frac{\rho}{r}\right]^3\right]\sin\frac{3\varphi}{2}\right\},$$

$$\sigma_\varphi = \frac{-K_{II}}{4\sqrt{2\pi r}}\left\{\left[3+2\frac{\rho}{r}+3\left[\frac{\rho}{r}\right]^2\right]\sin\frac{\varphi}{2}+\left[3+\frac{3}{2}\frac{\rho}{r}+\frac{15}{2}\left[\frac{\rho}{r}\right]^3\right]\sin\frac{3\varphi}{2}\right\}, \quad (12)$$

$$\tau_{r\varphi} = \frac{K_{II}}{4\sqrt{2\pi r}}\left\{\left[1+2\frac{\rho}{r}-3\left[\frac{\rho}{r}\right]^2\right]\cos\frac{\varphi}{2}+\left[3+\frac{9}{2}\frac{\rho}{r}-\frac{15}{2}\left[\frac{\rho}{r}\right]^3\right]\cos\frac{3\varphi}{2}\right\}.$$

Superimposing equations (8) and (12) the stress field in the vicinity of a drilled hole at the end of a slit may be described for general plane loading.

The Antiplane Problem

Because of the analogy between antiplane shear and plane potential flow, a starting function similar to the complex potential describing the flow past a circular cylinder is chosen:

$$F = A\,\xi^{\frac{1}{2}} + C\,\xi^{-\frac{1}{2}} = \phi(r,\varphi) + i\,\Psi(r,\varphi). \quad (13)$$

The complex variable ξ and the complex constants A, and C are defined by

$$\xi = x + iy = r\,(\cos\varphi + i\sin\varphi)\ ,\quad A = a + ib\ ,\quad C = c + id\ ,\quad i^2 = -1\ , \tag{14}$$

where a, b, c, and d are real undetermined constants. This yields

$$\phi(r,\varphi) = r^{\frac{1}{2}}\,[a\cos\tfrac{\varphi}{2} - b\sin\tfrac{\varphi}{2}] + r^{-\frac{1}{2}}\,[c\cos\tfrac{\varphi}{2} + d\sin\tfrac{\varphi}{2}]\ , \tag{15}$$

$$\Psi(r,\varphi) = r^{\frac{1}{2}}\,[a\sin\tfrac{\varphi}{2} + b\cos\tfrac{\varphi}{2}] - r^{-\frac{1}{2}}\,[c\sin\tfrac{\varphi}{2} - d\cos\tfrac{\varphi}{2}]\ . \tag{16}$$

To calculate the stress components the following definitions may be used:

$$\tau_{rz} = \frac{\partial\phi(r,\varphi)}{\partial r} = \frac{1}{r}\frac{\partial\Psi(r,\varphi)}{\partial\varphi}\ ,\quad \tau_{\varphi z} = \frac{1}{r}\frac{\partial\phi(r,\varphi)}{\partial\varphi} = -\frac{\partial\Psi(r,\varphi)}{\partial r}\ . \tag{17}$$

The boundary conditions for a slit ending in a drilled hole (Fig. 2)

$$\tau_{rz}(r = \rho) = 0\ ,\quad \tau_{\varphi z}(\varphi = \pm\,\pi) = 0\ , \tag{18}$$

and the comparison with equations (1), keeping in mind, that for the limiting case $\rho/r \longrightarrow 0$ the solution of the sharp crack equivalent is demanded, give:

$$a = c = 0,\quad b = -\frac{d}{\rho} = -\frac{2\,K_{III}}{\sqrt{2\pi r}}\ . \tag{19}$$

Thus, the stress field equations for the antiplane problem read:

$$\tau_{rz} = \frac{K_{III}}{\sqrt{2\pi r}}\left[1 - \frac{\rho}{r}\right]\sin\frac{\varphi}{2},\quad \tau_{\varphi z} = \frac{K_{III}}{\sqrt{2\pi r}}\left[1 + \frac{\rho}{r}\right]\cos\frac{\varphi}{2}\ . \tag{20}$$

DISCUSSION

The comparison between the Creager–equations (1) and the new field equations (8), (12) and (20) yields, that only the shapes of σ_φ on the ligament for mode I–loading are similar (Fig. 3), whereas, for mode II–loading the shapes of $\tau_{r\varphi}$ are clearly different (Fig. 4). The hoop stress distributions calculated with both, the new field equations (Fig. 5) and the Creager–equations (Fig. 6) for the respective notch shapes, show, that for notches with circular root equations (1) are approximately suitable to estimate the maximum notch stress for mode I–loading, but they are unfit to describe the whole stress field of such notches, especially for mixed mode– and mode II–loading. This is strengthened with the following comparisons of characteristic stress values:

– maximum notch stress for mode I–loading:

eqs (8): $\sigma_{max} = \sigma_\varphi\,(\varphi = 0^o;\ r = \rho) = 2.1213\,\dfrac{K_I}{\sqrt{\pi\rho}}$,

eqs (1): $\sigma_{max} = \sigma_\varphi\,(\varphi = 0^o;\ r = 0.5\,\rho) = 2\,\dfrac{K_I}{\sqrt{\pi\rho}}$,

– maximum shear stress for mode II–loading:

eqs (12): $$\tau_{max} = \tau_{r\varphi}\,(\varphi = 0^o;\ r = 1.723\ \rho) = 0.7132\,\frac{K_{II}}{\sqrt{\pi\rho}}\,,$$

eqs (1): $$\tau_{max} = \tau_{r\varphi}\,(\varphi = 0^o;\ r = 1.5\ \rho) = 0.3849\,\frac{K_{II}}{\sqrt{\pi\rho}}\,,$$

– maximum tangential stress on the notch surface for mode II–loading:

eqs (12): $$\sigma_{max} = \sigma_{\varphi}\,(\varphi = 67.115^o;\ r = \rho) = -\,2.8664\,\frac{K_{II}}{\sqrt{\pi\rho}}\,,$$

eqs (1): $$\sigma_{max} = \sigma_{t}\,(\varphi = 90^o;\ r = \rho) = -\,\frac{K_{II}}{\sqrt{\pi\rho}}\,,$$

– maximum shear stress for mode III–loading:

eqs (20): $$\tau_{max} = \tau_{\varphi z}\,(\varphi = 0^o;\ r = \rho) = 1.4142\,\frac{K_{III}}{\sqrt{\pi\rho}}\,,$$

eqs (1): $$\tau_{max} = \tau_{\varphi z}\,(\varphi = 0^o;\ r = 0.5\ \rho) = \frac{K_{III}}{\sqrt{\pi\rho}}\,.$$

Except for the maximum notch stress under mode I–loading the differences between all the characteristic stress values, calculated with both stress field equations, are distinct. Thus, the amount of stress concentration caused by a narrow notch is not only dependent on the notch root radius and the notch depth, but clearly on the notch shape, too. Therefore, it is recommended to use the new field equations as theoretical background for experimental and numerical investigations dealing with slits ending in a drilled hole or even U–shaped notches at least for mixed mode–, mode II– and mode III–loading.

REFERENCES

(1) Creager, M., "The elastic stress field near the tip of a blunt crack", Master's thesis, Lehigh University, 1966.
(2) Neuber, H., "Kerbspannungslehre", Springer Verlag, Berlin, 1985.

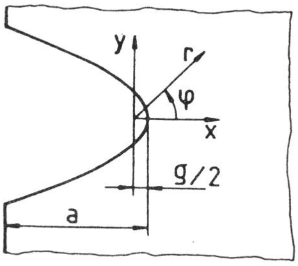

Fig. 1: Coordinate systems for Creager's stress field equations

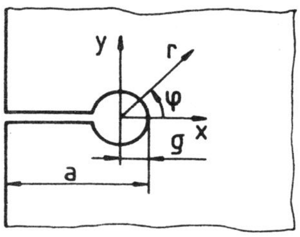

Fig. 2: Coordinate systems for the stress field at a slit ending in a drilled hole

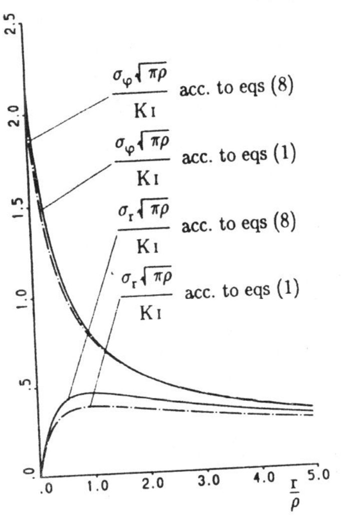

Fig. 3: Shapes of normal stresses on the ligament for mode I–loading

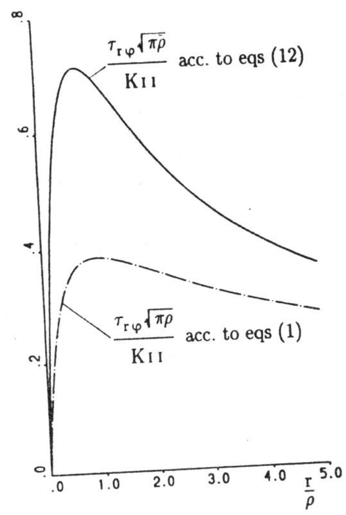

Fig. 4: Shapes of shear stress on the ligament for mode II–loading

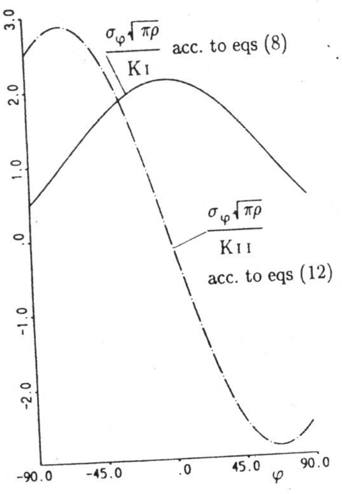

Fig. 5: Shapes of hoop stress for mode I– and mode II–loading for a slit ending in a drilled hole

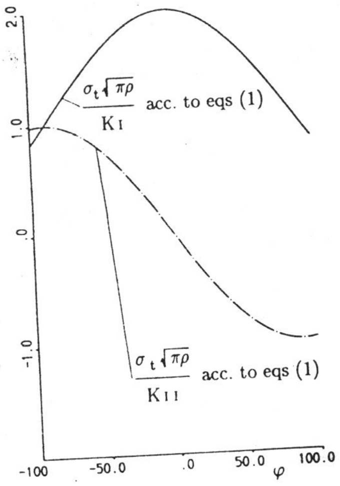

Fig. 6: Shapes of hoop stress for mode I– and mode II–loading for a parabolic notch.